Velocity-Selective Double Resonance: A Novel Technique for Determining Differential Scattering Cross Sections

Anthony J. McCaffery, Katharine L. Reid, and Benjamin J. Whitaker
School of Molecular Sciences, University of Sussex, Brighton BN1 9QJ, United Kingdom
(Received 8 August 1988)

The relationship between the velocity vectors of a gas-phase molecule before and after a collision is given by the differential cross section. Optical-optical double-resonance experiments using highly coherent sources can be used to obtain this information. Predictions and experimental considerations are discussed, and data are presented for elastic scattering in the $v=18$, $j=13$ level of $A\,^1\Sigma_u^+$-state Li_2 by Xe atoms.

PACS numbers: 33.40.Ta

One of the most sensitive probes of an intermolecular potential is the differential scattering cross section obtained by observation of the products of molecular collisions as a function of deflection angle. In the past, such studies have been possible only in crossed-molecular-beam experiments in which the species scattered from the collision center are monitored by rotatable detectors. The possible use of double-resonance line shapes to obtain information on differential cross sections has been discussed with regard to atomic collisions in a review article by Berman.[1] The first experimental demonstration that angular information could be obtained on molecular collisions in a thermal cell was given by Gottscho *et al.*[2] who used two counterpropagating laser beams. However, they were unable to extract differential cross sections.

In this Letter we demonstrate that by making full use of the velocity selection available with two very narrow line lasers, it is possible to extract differential cross sections in cell experiments. The principle of the method relies on the fact that sub-Doppler excitation of molecules results in not only a non-Maxwell-Boltzmann distribution of molecular speeds but also a nonisotropic distribution of molecular velocity directions relative to the laser axis. For example, exciting molecules at frequencies close to the center of the Doppler profile means that predominantly those moving perpendicular to the laser beam are selected. Similarly, molecules excited at frequencies towards the wings of the absorption profile move with a most probable velocity vector parallel to the laser beam.

Smith, Scott, and Pritchard[3] have shown that experiments on light molecules with a heavy atom as a collision partner ensure that for fast moving molecules these effects are dramatically carried across into the relative molecule-atom velocity distribution. Following these authors, we may write an expression for the probability of finding the magnitude, v_r, and the angle with respect to the laser axis, α, of the relative velocity vector for a given selected molecular velocity component v_L,

$$P(v_L,v_r,\alpha)=v_r^2\exp[-v_r^2\sin^2\alpha/2(s_a^2+s_m^2)]\times\exp[-(v_L-v_r\cos\alpha)^2/2s_a^2]\,, \quad (1)$$

where $s_x=(kT/m_x)^{-1/2}$ and the subscripts a,m denote atom and molecule. This equation has also recently been derived by us using an alternative approach.[4] Hence, we have information on the magnitude and direction of the relative velocity vector prior to collision.

A second laser, which probes the velocity distribution following collision, will thus be sensitive to changes in the relative velocity vector as a result of collision. The approach of Gottscho *et al.*[2] may be used to derive a relationship between the shift in velocity component, Δv_z, as a result of scattering and the center-of-mass scattering angle, θ_c (see Fig. 1),

$$\Delta v_z=v_L-v_{zf}=[m_a/(m_a+m_m)]v_r\cos\alpha(\cos\theta_c-1)\,, \quad (2)$$

where v_{zf} is the final velocity component. It is assumed that the change in internal energy is very small compared with the collision energy and that scattering out of the plane of Fig. 1 occurs isotropically. By making use of Eqs. (1) and (2) and a model probability, $P(\theta_c)$, of scattering occurring at θ_c, it is possible to predict the form of the double-resonance line shape if one also assumes that the first laser actually excites a Lorentzian distribution of velocity components, v_{zi}, about v_L. Thus the expression for the final line shape is a convolution of a Lorentzian with a scattering-angle–dependent function.

The system chosen for study was Li_2-Xe since it pro-

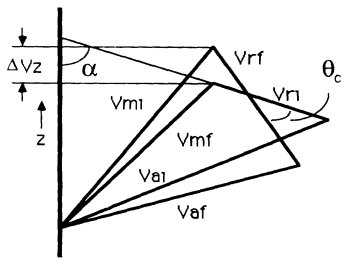

FIG. 1. The relationship between the change in the z component of molecular velocity Δv_{mz} and the center-of-mass-frame scattering angle θ_c. The subscripts are as follows: a, atom; m, molecule; r, relative; z, z component; i, initial; f, final.

vides a high atom-molecule mass ratio. Furthermore, Li_2 is known to have a number of accessible excited electronic states suitable for an optical-optical double-resonance experiment.[5] Lithium metal and Xe gas at a room-temperature pressure of 5 Torr were heated up to 930 K in a stainless-steel four-armed cell, each arm being fitted with quartz windows. Of the two lasers used in the experiment the first, L1, is a computer-controlled tunable ring dye laser operating with rhodamine 6G (Coherent model 699-29) pumped by an argon-ion laser (Coherent model Innova 100). This excites Li_2 from the $X\,^1\Sigma_g$ electronic state to the $A\,^1\Sigma_u$ electronic state. For the data presented later, the central frequency of the transition excited was 17040.29 cm^{-1} which corresponds to the transition from $v=3$, $j=12$ in the X state to $v=18$, $j=13$ in the A state. This was determined by our dispersing the red molecular fluorescence through a Czerny-Turner monochromator (Spex model 1402) to resolve the rovibronic structure. The second laser, L2, propagating antiparallel to the first, was a tunable ring dye laser (Coherent model 699-21) pumped by 6 W of argon-ion radiation (Spectra Physics model 165) on all lines, and controlled by a microcomputer (Atari model 1040ST) to enable scans of up to 30 GHz. For L2, the frequency used was 17016 ± 1 cm^{-1} as determined by a fiber-optic-coupled wave meter (Burleigh model Junior). This transition has not been assigned (and could possibly result from the absorption of more than two photons) but almost certainly corresponds to reexcitation from $v=18$, $j=13$ in the A state (i.e., no energy transfer has occurred). The fluorescent light was collected orthogonally to the excitation axis and focused onto a photomultiplier tube (EMI model 9635 QB, S11 spectral response) and filtered (Corning UG11) to remove the A-X emission.

Velocity-resolved double-resonance line shapes were obtained by phase-sensitive detection of the total uv-blue fluorescence at the frequency used to chop L1, as a function of the wavelength of L2 with L1 kept fixed at a point on the X-A absorption profile. The observed signal must therefore result from the absorption of at least one photon from each laser.

L1 was scanned over 20 GHz to locate the approximate line center of the X-A absorption profile. With L1 kept fixed at this location, L2 was scanned over 5 GHz. This produced the most intense absorption profile in Fig. 2. L1 was then offset in steps of 0.2 GHz and L2 scanned to produce the other profiles illustrated in this figure. Inspection of the data suggests that the first scan did not correspond to the exact center of the X-A transition. To compensate for this, an estimate was made by measurement of the line intensities as to where the real line center occurred in terms of the frequency of L1. This frequency, which may be ± 0.1 GHz (~ 50 ms^{-1}), was then assigned as the zero-velocity-component point. The Doppler formula was then employed to assign velocities to the other L1 frequencies used in the subsequent scans.

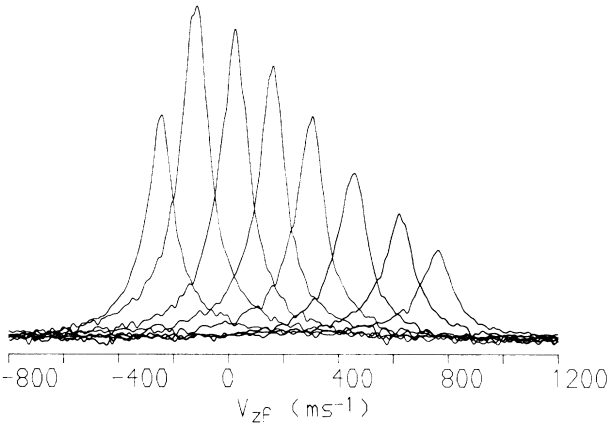

FIG. 2. Total fluorescence profiles resulting from the absorption of at least one photon from each of L1 and L2 as a function of final velocity component, v_{zf}, for L1 offset in steps of 0.2 GHz (117.6 ms^{-1}).

A Levenberg-Maquard algorithm[6] was used to make an approximate Lorentzian[1] $\{L(x)=\gamma/[(x-x_0)^2+\gamma^2/4]\}$ fit to the double-resonance line-shape that resulted from putting L1 nearest to the line center. This was in order to find an approximate half-width, γ, the result being 138 ms^{-1}. In this preliminary work, pressure- and power-broadening studies have not been carried out, and although the origin of the Lorentzian is unimportant some of its width will be due to the velocity vector changing direction on collision, so that this width will be wider than that of the homogeneous line shape common to all scans. A half-width slightly smaller, 129 ms^{-1}, to allow for this and to compensate for the fact that this profile does not result from the true line center, was then used to generate the line shape for the predictions at velocities corresponding to other laser excitation frequencies.

Figure 3 compares the limiting cases of totally forward scattering, $P(\theta_c)=\delta(\theta_c-0)$, and isotropic scattering, $P(\theta_c)=1$, with the experimental data and with a predicted line shape for $P(\theta_c)=\theta_c^2\exp(-k\theta_c^2)$ with $k=6.25\times10^{-4}$, an energy-independent function which peaks at 40°. This last function was chosen because it ties in reasonably well with experiment and calculations[7,8] and peaks at the angle found to be the most probable for the experimental line shape in Fig. 3. Preliminary work suggests that the difference between the predicted line shape using this function and the experimental line shape in Fig. 3 is related to the actual functional form and energy dependence of the differential cross section. However, it has not yet been possible to test this quantitatively because of lack of information on homogeneous-line-broadening effects. All figures are shown for $v_L=371$ ms^{-1}, $\gamma=129$ ms^{-1}, and a temperature of 930 K. The convention used is that the second laser defines the positive z direction. These results are summarized in Table I.

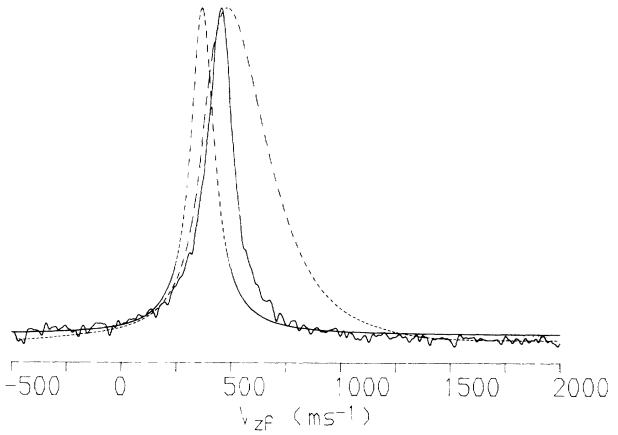

FIG. 3. Three predicted line shapes as functions of v_{zf} are shown for $v_L = 371$ ms^{-1}, $\gamma = 129$ ms^{-1}, and temperature $= 930$ K with $P(\theta_c) = \delta(\theta_c - 0)$ (dash-dotted line), $P(\theta_c) = 1$ (dotted line), and $P(\theta_c) = \theta_c^2 \exp(-6.25 \times 10^{-4} \theta_c^2)$ (i.e., a function peaking at 40° independent of energy) (dashed line) and compared with the experimental data for this v_L (solid line).

The results indicate that the elastic collisions studied here are predominantly forward scattered. It is useful to note that if the relative velocity distribution were very peaked (not true for the cases presented here), then any angular information would relate to a narrow range of collision energies. However, even for the data in the table, the scattering angle relates to a spread of collision energies which is smaller than the thermal spread and centered on $\mu v_{rp}^2/2$, where μ is the reduced mass. This means that we have a handle on the energy dependence of the most probable scattering angle, something previously unattainable without the use of molecular beams.

We believe that it is feasible to study rotationally inelastic collisions in this manner and we expect to see larger line-broadening effects in some of these cases. It is evident that fairly detailed scattering-angle information, including its energy dependence, may be extracted. We are also interested in the polarization of the A-X emission after rotational energy transfer has occurred[9] to see how this compares with scattering-angle information; in the experiment, the relation between the vectors **j** and **v**$_r$ changes across the absorption profile.

TABLE I. The velocity component, v_L, most probably excited for a given laser offset (central frequency 17040.29 cm^{-1}). The other symbols are as follows: v_{zfp}, the most probable final velocity component; Δv_z, the velocity component shift $(v_L - v_{zf})$; v_{rp}, the most probable relative speed selected; α_p, the most probable angle between the laser axis and the relative velocity vector; θ_{cp}, the most probable energy-averaged center-of-mass scattering angle deduced from the other quantities.

Offset (GHz)	v_L (ms^{-1})	v_{zfp} (ms^{-1})	Δv_z (ms^{-1})	v_{rp} (ms^{-1})	α_p (deg.)	$v_{rp}\cos\alpha_p$ (ms^{-1})	θ_{cp} (deg.)
0.2	−216	−244	28	817	106	−225	30
0.0	−99	−120	21	793	98	−110	38
−0.2	18	23	−5	788	88	28	35
−0.4	136	159	−23	799	80	139	35
−0.6	254	299	−45	829	72	256	36
−0.8	372	451	−79	877	64	384	39
−1.0	489	619	−130	941	58	499	45
−1.2	617	756	−139	1016	53	611	42

The support of the Science and Engineering Research Council is gratefully acknowledged.

[1]P. R. Berman, Adv. At. Mol. Phys. **13**, 57 (1977).

[2]R. A. Gottscho, R. W. Field, R. Bacis, and S. J. Silvers, J. Chem. Phys. **73**, 599 (1980).

[3]N. Smith, T. P. Scott, and D. E. Pritchard, J. Chem. Phys. **81**, 1229 (1984).

[4]C. P. Fell, A. J. McCaffery, K. L. Reid, A. Ticktin, and B. J. Whitaker, Laser Chem. (to be published).

[5]R. A. Bernheim, L. P. Gold, P. B. Kelly, C. Tomczyk, and D. K. Veirs, J. Chem. Phys. **74**, 3249 (1981).

[6]J. E. Dennis and R. B. Schnabel, *Numerical Methods for Unconstrained Optimisation and Non-Linear Equations* (Prentice Hall, Engelwood Cliffs, NJ, 1983).

[7]J. A. Serri, C. H. Becker, M. B. Elbel, J. L. Kinsey, W. P. Moskowitz, and D. E. Pritchard, J. Chem. Phys. **74**, 5116 (1981).

[8]J. A. Serri, R. M. Bilotta, and D. E. Pritchard, J. Chem. Phys. **77**, 2940 (1982).

[9]A. J. McCaffery, M. J. Proctor, E. A. Seddon, and A. Ticktin, Chem. Phys. Lett. **132**, 185 (1986).